Research Square

Preprints are preliminary reports that have not undergone peer review.
They should not be considered conclusive, used to inform clinical practice,
or referenced by the media as validated information.

Non-random defaunation across China's protected area network revealed by multidimensional dark diversity

Chenyang Zhu
Kunming Institute of Zoology
Zhechang Hu
Kunming Institute of Zoology
Mingwei Yang
Kunming Institute of Zoology
Yang Liu
Kunming Institute of Zoology
Kenneth Otieno Onditi
Kunming Institute of Zoology
Hongjiao Wang
Kunming Institute of Zoology
Xuelong Jiang
Kunming Institute of Zoology
Xueyou Li
lixueyou@mail.kiz.ac.cn

Kunming Institute of Zoology

Article

Keywords: camera trapping, community completeness, conservation gap analysis, functional diversity, phylogenetic diversity, protected-area effectiveness, terrestrial mammals

Posted Date: August 5th, 2026

DOI: https://doi.org/10.21203/rs.3.rs-10531544/v1

License: This work is licensed under a Creative Commons Attribution 4.0 International License.
Read Full License

Additional Declarations: No competing interests reported.

Non-random defaunation across China's protected area network revealed by multidimensional dark diversity

Chenyang Zhu[1,2], Zhechang Hu[1,2], Mingwei Yang[1,2], Yang Liu[1], Kenneth Otieno Onditi[1], Hongjiao Wang[1], Xuelong Jiang[1*], Xueyou Li[1*]

[1]State Key Laboratory of Genetic Evolution and Animal Models & Yunnan Key Laboratory of Biodiversity and Ecological Conservation of Gaoligong Mountain, Kunming Institute of Zoology, Chinese Academy of Sciences, Kunming, Yunnan 650201, China

[2]Kunming College of Life Sciences, University of Chinese Academy of Sciences, Kunming, Yunnan 650201, China

[*] For correspondence: jiangxl@mail.kiz.ac.cn (XJ); lixueyou@mail.kiz.ac.cn (XL)

Abstract

Protected areas are central to global biodiversity conservation, yet assessments of their effectiveness focus largely on observed species richness. This approach overlooks dark diversity—the species absent from biogeographically suitable habitats and their associated evolutionary and ecological roles. We used a dataset comprising 7.4 million camera-trap days across 199 nature reserves in China to assess the taxonomic, phylogenetic, and functional dark diversity of medium- and large-sized mammals. On average, protected areas were missing more than half of the mammal species expected under their environmental conditions (mean adjusted taxonomic dark diversity = 0.56), revealing pervasive community incompleteness across the national reserve network. Phylogenetic dark diversity indicated substantial losses of evolutionary history (mean expected deficit = 468 Myr), while functional dark diversity showed widespread deficits in ecological trait space. A biogeographic null-model analysis revealed that these deficits were strongly non-random, with South China exhibiting significantly elevated taxonomic, phylogenetic, and functional dark

diversity relative to null expectations. The three dimensions were positively correlated but captured complementary conservation signals: taxonomic dark diversity was primarily associated with reserve area, sampling effort, and governance context; phylogenetic dark diversity reflected elevation, topographic heterogeneity, precipitation, and productivity; and functional dark diversity was linked to historical defaunation interacting with regional trait-space constraints. Species absent from otherwise suitable reserves were disproportionately threatened, dietary specialists, and cathemeral or crepuscular mammals, indicating trait-selective defaunation. Together, our results show that China's protected areas are often incomplete remnants of historically richer mammal communities and that assessments based on species richness alone substantially underestimate biodiversity erosion. Integrating taxonomic, phylogenetic, and functional dark diversity into protected-area evaluation provides a powerful framework for identifying hidden conservation debt, prioritizing restoration and connectivity, and advancing biodiversity recovery under the Kunming–Montreal Global Biodiversity Framework.

Keywords: camera trapping, community completeness, conservation gap analysis, functional diversity, phylogenetic diversity, protected-area effectiveness, terrestrial mammals

Introduction

Unprecedented human activity has triggered a global change crisis that jeopardizes ecosystem stability and human well-being [1–3]. Protected areas (PAs) represent the primary strategy to combat these declines [4,5], a role recently reinforced by the Kunming-Montreal Global Biodiversity Framework's commitment to protect 30% of terrestrial and marine environments by 2030 [6]. Despite this policy momentum, empirical evaluations of PA effectiveness in preventing local extinctions remain limited and prone to methodological bias [7]. Current evaluation frameworks rely predominantly on absolute, observed local species richness to gauge success [7–9]. This reliance on raw richness presents a critical limitation: it conflates true protection effects with baseline habitat quality—the inherent ecological potential of a site—obscuring or artificially inflating actual

conservation performance [10,11]. Consequently, reserves exhibiting identical species counts may diverge markedly in their realization of regional ecological potential, skewing restoration priorities and management strategies [11,12]. Addressing these theoretical and applied challenges requires moving beyond quantifying observed local diversity to characterize the portion of biodiversity that is currently absent but could theoretically be supported by a given site.

Dark diversity refers to the set of species that are absent from a focal site but are ecologically compatible with its biogeographical, historical, and environmental conditions and could potentially establish under suitable circumstances [10,13,14]. Unlike observed diversity, which reflects only the realized component of communities, dark diversity provides a measure of community incompleteness by quantifying the gap between current assemblages and their potential composition [15]. Estimating dark diversity typically requires integrating regional species pools with information on species-specific ecological requirements, environmental conditions, and biotic interactions to identify species that are compatible with, but currently missing from a given site [10,14]. This approach provides a direct assessment of biodiversity deficits relative to ecological potential, offering a more informative benchmark for evaluating conservation outcomes than observed species richness alone [14]. Importantly, dark diversity can reveal whether biodiversity losses are random or structured, distinguishing stochastic absences from systematic declines driven by habitat degradation, anthropogenic pressures, dispersal limitation, or historical extirpations [15,16]. By identifying missing but potentially recoverable species, dark diversity provides a powerful framework for prioritizing restoration, guiding species reintroductions, and evaluating the functional completeness and resilience of protected area networks [11,17]. For example, two protected areas may support similar observed mammal richness, yet differ markedly in their ecological completeness [18,19]. A reserve located in an intact landscape may exhibit low dark diversity, indicating that most species capable of inhabiting the site are already present [11]. In contrast, another reserve with the same observed richness but a much larger dark diversity may have experienced

historical extirpations or ongoing anthropogenic pressures [18], leaving many ecologically suitable species absent from the community. By revealing these hidden deficits, dark diversity can distinguish communities that are naturally species-poor from those that are impoverished relative to their ecological potential [11], thereby providing a critical basis for identifying restoration priorities and targeting species recovery actions. Additionally, taxonomy alone cannot capture the multidimensional nature of community incompleteness: species also carry phylogenetic histories and functional roles whose absence reshapes ecosystems [17,20,21]. Recent work shows that defaunation of threatened species disproportionately affects specific lineages and functional groups, driving phylogenetic and functional homogenization—patterns that remain invisible to richness-based metrics [22–25]. Therefore, integrating functional and phylogenetic dimensions of dark diversity alongside taxonomic measures is essential for revealing hidden losses of ecological functions and evolutionary history, and for providing a more comprehensive assessment of ecosystem integrity and conservation priorities.

Dark diversity is not merely a reflection of biodiversity loss but emerges from the interplay between species-specific constraints and site-specific ecological filters [15,26]. At the species level, traits such as dispersal ability, habitat specialization, and dietary requirements can determine whether species are able to colonize and persist in otherwise suitable environments [3,27]. Incorporating functional traits into assessments of dark diversity can therefore provide critical insights into the mechanisms underlying species absences, allowing researchers to distinguish between missing species that are unlikely to establish naturally and those whose ecological functions could potentially be restored [15]. Accounting for functional characteristics is essential for interpreting dark diversity as a measure of deterministic community assembly processes and for identifying the functional potential that ecosystems can realistically support, thereby informing more effective conservation and restoration strategies [11].

At the site level, dark diversity can be shaped by both natural and anthropogenic processes, including dispersal limitation, biotic interactions such as competitive exclusion, environmental filtering, habitat fragmentation, and historical land-use changes [11]. Conservation interventions, including the establishment and management of protected areas, may also influence dark diversity by modifying habitat conditions, connectivity, and extinction risks [18,19]. To understand why particular species are absent from sites where they could potentially occur, it is therefore crucial to disentangle species-driven and site-driven mechanisms [15]. Without explicitly accounting for these interacting drivers, estimates of dark diversity may confound species-level limitations with site-level deficiencies, potentially obscuring the ecological processes responsible for community incompleteness [15].

Medium and large-sized mammals (>1 kg) provide an ideal system for investigating multidimensional dark diversity because of their disproportionate ecological roles, sensitivity to environmental change, and increasing availability of large-scale distribution data [22–24]. Their large home ranges, low densities, and elusive behaviours also make them prone to local extirpation before declines become evident in observed species richness, generating extinction debts that may persist for decades [25,28,29]. Meanwhile, the rapid expansion of camera-trap networks enables standardized assessments of mammal occupancy and community composition across continental scales [30–32]. Despite increasing applications of dark diversity, most studies have focused on its taxonomic dimension [18,19], with limited efforts to incorporate species traits and site characteristics or to test whether community incompleteness reflects non-random losses at biogeographic scales [33,34]. Such non-random patterns are particularly important for conservation because they reveal whether missing species represent structured losses of functional strategies, evolutionary lineages, or ecological processes rather than simple stochastic absences. China offers a unique opportunity to address these questions, as it spans the Palearctic and Oriental realms, contains four global biodiversity hotspots, and supports a diverse medium- and large-sized mammal fauna (236 species

131 in 39 families) [35,36]. Although a national protected-area network now covers more than 18% of
132 China's terrestrial area [37,38], it remains unclear whether these reserves harbour mammal assemblages
133 that match their ecological potential or whether they represent structurally intact but functionally
134 depleted ecosystems due to historical and ongoing defaunation.
135
136 Here, we integrate 7.4 million camera-trap days from 199 terrestrial reserves across China with
137 comprehensive phylogenetic and functional-trait databases for medium- and large-sized mammals
138 to address four questions: (i) What are the spatial patterns of taxonomic, phylogenetic, and
139 functional dark diversity across China's reserve network? (ii) Which environmental, anthropogenic,
140 and methodological factors drive each dimension? (iii) Does dark diversity deviate non-randomly
141 from null expectations across zoogeographic regions, and if so, in which dimensions? (iv) Are
142 different dimensions of community incompleteness coupled or do they provide complementary
143 conservation signals? We hypothesize that: **(H1)** observed species richness may underestimate
144 biodiversity deficits because anthropogenic pressures can selectively remove sensitive mammals
145 while maintaining superficially intact richness [23,28,39,40], resulting in a decoupling between observed
146 diversity and multidimensional community completeness. This decoupling should be strongest in
147 regions with long-term human impacts. **(H2)** the three dimensions of dark diversity are regulated
148 by distinct ecological mechanisms, resulting in dimension-specific patterns of environmental and
149 anthropogenic drivers. **(H3)** dark diversity should exhibit non-random patterns because mammal
150 losses are structured by species traits and evolutionary history [40–43]; therefore, functional and
151 phylogenetic dimensions are expected to show stronger deviations from random expectations than
152 taxonomic diversity. **(H4)** these processes should generate region-specific combinations of
153 biodiversity deficits, reflecting variation in climate, topography, and human land-use history across
154 China's zoogeographic regions. By integrating taxonomic, functional, and phylogenetic
155 perspectives, this study provides a comprehensive assessment of mammal community

incompleteness and establishes a framework for translating large-scale biodiversity monitoring into actionable conservation priorities.

Methods

Study system and reserve network

China spans 73.5°–135.1°E and 3.9°–53.6°N, encompassing tropical, subtropical, temperate and boreal biomes with a precipitation gradient from >2000 mm in the southeast to <50 mm in the northwest and an elevational range from sea level to over 6000 m on the Qinghai-Tibet Plateau [44,45]. It harbours four global biodiversity hotspots — the Mountains of Southwest China, Indo-Burma, Himalaya and Mountains of Central Asia [46]. Following Zhang[47], we partitioned reserves into seven zoogeographic regions: South China, Central China, Mongolian-Xinjiang, Southwest China, Northeast China, Qinghai-Tibet, and North China. China's national reserve network is regulated by the *Regulations of the People's Republic of China on Nature Reserves* (1994, revised 2017) and, since 2019, is being progressively reorganized under a unified national park system spanning national parks, nature reserves *sensu stricto* and nature parks [37]. By 2023, more than 11,800 protected areas of various levels — national, provincial, municipal and county — cover ≈18% of the terrestrial territory, but coverage and management intensity are strongly biased east-west: the humid eastern and southern provinces host the largest number of small-to-medium reserves under strong anthropogenic pressure, whereas the arid, cold and topographically extreme western and northwestern regions contain fewer but much larger reserves (e.g.Sanjiangyuan, Kekexili) that are demographically sparse and less human-influenced [37,38].

Camera-trap dataset

We searched the China National Knowledge Infrastructure (CNKI), Web of Science and Scopus through June 2025 for camera-trap studies in Chinese terrestrial nature reserves using the keywords "camera trap" and "红外相机". After excluding studies that (i) used baited cameras, (ii) did not

provide a complete species list, or (iii) reported fewer than 400 effective camera-days per survey [48], we retained 421 publications spanning 256 reserves. To ensure that dark-diversity estimates were not driven by low-effort surveys, we further restricted the analytical dataset to reserves with >30 deployed camera stations and >400 effective camera-days, yielding a final network of 199 reserves with >7.4 million effective trap-days (Appendix S1).

We restricted analyses to medium- and large-sized mammals (mean adult body mass >1 kg) [36,48] and excluded arboreal species (gibbons, flying squirrels) that are poorly detected by ground-level cameras. The retained dataset contained 105 species in 8 orders and 22 families; 79 (75%) are nationally key protected wildlife and 65 (62%) are listed as threatened in the China Red List of Mammals [49].

Reserve-level species pools

A defensible species pool is the cornerstone of any dark-diversity analysis [10,50,51]. We constructed reserve-specific pools through a three-step spatial filter of the IUCN Red List range polygons (https://www.iucnredlist.org). First, polygons were intersected with each species' published habitat affiliations using the global habitat-type layer of Jung et al.[52] Second, the resulting polygons were further filtered by IUCN elevational limits using the SRTM4 90-m digital elevation model. Third, the refined polygons were overlaid on each reserve's boundary (NSII national platform; circular equal-area buffers were used where vector boundaries were unavailable) to derive a binary reserve × species presence/potential matrix. To capture the historical footprint of the fauna and reduce the risk that recent range contractions eroded the effective pool, we further integrated historical distribution records for each species from the China Endangered Species Information System (CESIS; via Map of Life, mol.org) following Liu et al.(2025) [53]: each historical occurrence was buffered by a 50-km radius, and the union with the modern IUCN polygon was retained as the potential range. The pool was restricted to terrestrial, ground-dwelling species with mean adult

body mass >1 kg, matching the taxonomic scope of the observed communities and excluding arboreal taxa (gibbons, flying squirrels) that ground-level cameras do not reliably detect. This produced a macroclimatic-, historical- and habitat-filtered pool consistent with current best practice [54,55].

Environmental and trait predictors

For each reserve, we extracted the following environmental and anthropogenic variables: Elevation and elevational range (derived from SRTM; at 90 m resolution, https://srtm.csi.cgiar.org): elevation captures the thermal and vegetation-structural regime that filters mammalian communities along altitudinal gradients, and ER within each reserve is a proxy for topographic heterogeneity, which enlarges the local niche space and buffers species against climatic extremes [56,57]. Annual mean precipitation (obtained from WorldClim 1.4 at ~1 km resolution, https://www.worldclim.org); it correlates with primary productivity and, in China, is a first-order predictor of vegetation structure and prey availability. Global Human Modification index (derived from gHM 2016 v1 at ~1 km resolution, https://sedac.ciesin.columbia.edu); it integrates the cumulative footprint of built-up land, cropping, roads, mining, energy infrastructure and human population, capturing the anthropogenic pressure that removes sensitive mammals Net primary productivity (NPP, derived from MOD17A3HGF v061 at ~1 km resolution, https://lpdaac.usgs.gov); it approximates energy input at the base of the food web, on which mammalian carrying capacity depends [58]. Landscape patch density (PD), derived from ESA WorldCover 10 m land-cover map (https://esa-worldcover.org) using R package landscapemetrics, indexes habitat fragmentation. Reserve area (from the National Specimen Information Infrastructure, http://www.nsii.org.cn, with reserve boundary shapefiles; for the small subset of reserves that lacked a digitized boundary, a circular buffer of equivalent area was constructed around the reported centroid) enters the site-level model as log(AREA + 1) after z-standardization, capturing the carrying-capacity effect that mediates edge-driven extinction filtering. Year of reserve establishment (es_time) captures the duration of formal protection, which

conditions post-establishment recovery of persecuted taxa. Protected-area level (national, provincial, municipal, county) captures governance intensity, which modulates enforcement of anti-poaching and land-use rules. To control for detection bias, we included log-transformed effective camera-trap days (logTRAPDAY). Following pre-filtering to >30 cameras per reserve, Pearson correlation screening ($|r| > 0.7$) led to removal of mean temperature, which was highly collinear with precipitation.

Three dimensions of dark diversity

Taxonomic dimension (DD_{adj}). Following Carmona & Pärtel [54], we used the hypergeometric co-occurrence approach. For every species pair (i, j), the standardized effect size of observed co-occurrence relative to the null hypergeometric expectation across the 199 reserves was computed as $SES_{ij} = (M_{ij} - \bar{M}_{ij})/\sqrt{Var_{ij}}$ and aggregated into an indication matrix. For a focal absent species i in reserve k with observed species set S_k, the probability of belonging to dark diversity was obtained by summing weighted SES values and back-transforming with the standard normal CDF [59]. Reserve-level dark diversity was the sum of probabilities, and the adjusted index $DD_{adj} = DD/m$ (where m = pool size) was used to enable cross-reserve comparison [60].

Phylogenetic dimension (EPD). We adapted Faith's [20] expected phylogenetic diversity framework to dark diversity. Branches were taken from the Upham et al.[61] DNA-only, node-dated, birth-death completed mammal phylogeny for 5911 species (constrained to a resolved backbone topology; downloaded from vertlife.org). To propagate phylogenetic uncertainty, all phylogenetic dark-diversity metrics were recomputed on 200 posterior trees randomly sampled from the 10000-tree posterior distribution and the per-reserve mean and 95% quantile were retained. On each tree, each branch j of length Lj with descendant set Sj was assigned a probability of dark occupation $q_{jk} = 1 - \prod_{i \in S_j}(1 - p_{ik})$, where pik is the dark-diversity probability of species i in reserve k (zero for

species already observed). Reserve-level expected phylogenetic dark diversity was $EPD_k = \sum_j L_j\, q_{jk}$.

Functional dimension (FDI). A Gower-distance trait space was constructed from four traits: adult body mass (log10-transformed) and diet composition, both taken from the EltonTraits 1.0 database[62]; diel activity pattern (diurnal, nocturnal, crepuscular, cathemeral) and IUCN threat status (threatened: VU/EN/CR vs. non-threatened: LC/NT), both taken from Jiang et al.[63] Diet was recoded into three categories following Atwood et al.[64]: carnivore (>=90% animal), herbivore (>=90% plant), otherwise omnivore. Functional metrics were computed via FD::dbFD with Cailliez correction of the Gower matrix and the maximum number of principal coordinate axes retained (m = 'max'; equivalent to species-pool size minus one when it does not exceed the number of trait dimensions). Functional richness (FRic) was computed for observed and observed+dark species sets within a single global functional space [17]. The functional deficit index was $FDI = (FRic_{obsUdark} - FRic_{obs})/FRic_{obsUdark}$, quantifying the proportion of the potential trait space currently unfilled. Functional dispersion of the dark assemblage (FDis_dark) was also computed as a complementary structural metric.

For both EPD and FDI/FDis_dark we computed standardized effect sizes (SES_EPD, SES_FDis_dark) against 999 reserve-level random draws that preserved the number of absent species per reserve, isolating non-random concentration on particular phylogenetic branches or trait regions.

Drivers of dark diversity

Bayesian species–site unified model. Following Fujinuma & Pärtel, we partitioned dark-diversity affinity (DDA ∈ [0,1]) into a species component (dda_sp, regressed against traits) and a site component (dda_site, regressed against reserve characteristics):

$$logit\left(dda_{sp}\right) = \alpha_{sp} + \sum_{k=1}^{K} \beta_{sp.k} . \mathrm{T}_k$$

$$logit(dda_{site}) = \alpha_{site} + \sum_{m=1}^{M} \beta_{site.m} . \mathrm{E}_m$$

$$logit(DDA) = \frac{logit\left(dda_{sp}\right) + logit(dda_{site})}{2}$$

The realized occurrence matrix was fitted as Bernoulli(p) with $logit(p) = logit\big((1 - DDA) * suit\big) + \delta$, where δ calibrates the average prevalence. Three MCMC chains were run in *rjags* [65], each retaining 333 post–burn-in samples (999 posterior draws in total). Convergence was declared when Gelman-Rubin $\hat{R} \leq 1.05$ for all monitored parameters.

Spatially explicit GAMs. For EPD, SES_EPD, FDI, FDis_dark and SES_FDis_dark we built spatially explicit generalized additive models (Gaussian or Beta family as appropriate, including a tensor smoother s(longitude, latitude, k = 20) to absorb residual spatial autocorrelation), and conducted backward selection with AIC. All continuous predictors entered as thin-plate smooths (k = 4). Moran's I residual tests confirmed that the spatial smoother removed large-scale autocorrelation in every model.

Regional null-model tests of biogeographic non-randomness

The drivers above identify covariates of dark diversity but do not test whether community incompleteness departs from chance at biogeographic scale. To address this question, for each of

the three dimensions (DD_{adj}, EPD, FDI) we ran a regional permutation null model. In each of 9999 permutations, reserve-level dark-diversity values were randomly reshuffled across the 199 reserves (preserving the number of reserves per zoogeographic region), and the regional mean was recomputed.

$$SES_{region} = (mean_{obs} - mean_{null})/SD_{null}$$

The standardized effect size quantifies the directional deviation; two-tailed P-values were obtained from the empirical permutation distribution and adjusted across regions using the Benjamini–Hochberg false-discovery-rate procedure. A region was classified as significantly impoverished (SES > 0, more potential species missing than expected — "higher than null") or significantly retained (SES < 0, fewer absent species than expected — "lower than null") when adjusted $P < 0.05$. To our knowledge, this is the first study to conduct an explicit biogeographic null-model assessment across all three dimensions of dark diversity simultaneously.

Multidimensional couplings

Spearman rank correlations among observed species richness (SR), DD_{adj}, EPD and FDI were computed across the 199 reserves, and visualized with a scatter–density matrix.

All analyses were performed in R v4.4.1 (R Core Team 2024) with the following packages: rjags 4-16 (with JAGS 4.3.1) for the Bayesian species-site model; mgcv 1.9.1 for the spatial GAMs; FD 1.0-12.3 for functional dispersion and functional richness; picante 1.8.2 and ape 5.8-1 for phylogenetic metrics; phytools 2.4-4 and phangorn 2.12.1 for tree manipulation; landscapemetrics 2.2.0 for landscape patch density; terra 1.8-29 for raster processing; vegan 2.6-4 for data standardisation (decostand); spdep 1.3-4 for spatial autocorrelation diagnostics; and dplyr 1.1.4, ggplot2 4.0.2, patchwork 1.3.2 and ragg 1.4.0 for data handling and figure production.

Results

PA network coverage and species composition

The 199 reserves spanned every major biogeographic zone of China, with extensive coverage in Southwest, Central and South China and sparser representation of Qinghai-Tibet and Mongolian-Xinjiang (Fig. 1). The 105 recorded medium- and large-sized mammal species belonged to 8 orders, with Carnivora the most species-rich (42 spp., 40.0% of total), followed by Cetartiodactyla (33 spp., 31.4%), Primates (9), Lagomorpha (8), Rodentia (7), Perissodactyla (3), Pholidota (2) and Proboscidea (1). Per-reserve observed richness ranged from 2 to 30 species (mean = 12.4 ± 5.5 SD).

Multidimensional spatial structure of dark diversity

Adjusted taxonomic dark diversity (DD_{adj}) ranged from 0 to 0.95 across reserves (mean = 0.56 ± 0.15), implying that on average more than half of the ecologically suitable medium- and large-sized mammal species were absent from each reserve (Fig. 2a). High values were concentrated in the southern hill country, the southern margin of the Hengduan Mountains and southeastern coastal reserves; values were lowest on the Qinghai-Tibet Plateau and in parts of North and Northeast China.

Expected phylogenetic dark diversity (EPD; branch-length units) ranged from 158 to 854 Myr across reserves (mean = 468 ± 135 Myr) and the functional deficit index (FDI) ranged from 0 to 0.88 (mean = 0.22 ± 0.17), both displaying spatial structures broadly congruent with DD_{adj} — maxima in southern and parts of central-eastern China, minima on the Qinghai-Tibet Plateau and in the north (Fig. 2b, c).

Observed species richness (SR) was strongly negatively correlated with the taxonomic and functional dimensions (Spearman $\rho_SR–DD_{adj} = -0.60$, $P < 0.001$; $\rho_SR–FDI = -0.61$, $P < 0.001$) but was decoupled from the phylogenetic dimension ($\rho_SR–EPD = -0.04$, $P = 0.62$), indicating

that lineage-level incompleteness scales with pool depth rather than with per-site richness (Fig. 5, Fig. S2). The three dark-diversity dimensions were positively correlated with one another (ρ_DD_{adj}–EPD = +0.69, ρ_DD_{adj}–FDI = +0.74, ρ_EPD–FDI = +0.44; all $P < 0.001$), but all inter-dimensional correlations fell well below unity, confirming coupled but non-redundant information content.

Drivers of taxonomic dark-diversity affinity (Bayesian species–site unified model)

The Bayesian species–site unified model converged for all parameters (Gelman-Rubin $\hat{R} \leq 1.05$) and identified six *site-level* covariates whose 95% credible intervals excluded zero (Fig. 3a). Reserve area (posterior mean β = −0.34, 95% CrI [−0.494, −0.203]) and sampling effort (logTRAPDAY; β = −0.27, [−0.378, −0.158]) both significantly *reduced* site-level dark-diversity affinity, and Municipal-level reserves carried a strongly negative intercept (β = −0.79, [−1.40, −0.16]) relative to the reference administrative level. Zoogeographic-region intercepts were heterogeneous: Southwest China (β = +0.91, [+0.32, +1.49]) and North China (β = +0.44, [+0.10, +0.80]) had significantly *positive* intercepts, while South China had a significantly *negative* intercept (β = −0.38, [−0.75, −0.01]) — meaning that once reserve area, sampling effort and administrative level are partialled out, the raw southern excess in dark diversity is fully absorbed by these reserve-level covariates rather than by a regional constant. Annual precipitation, elevation, elevational range, gHM, NPP, and landscape patch density (PD) were not significant after partialling the retained covariates.

At the *species* level (Fig. 3b), nine trait effects had 95% credible intervals excluding zero. IUCN Threatened status was the single strongest positive predictor (β = +1.21, [+1.10, +1.33]), with the mirror-image non-threatened baseline correspondingly negative (β = −1.21, [−1.33, −1.10]). Along the diet axis, herbivorous (β = +0.83, [+0.66, +1.00]) and carnivorous (β = +0.35, [+0.15, +0.55]) species carried significantly higher dark-diversity affinity than omnivores, which were themselves

significantly retained (omnivorous β = −1.18, [−1.33, −1.02]). Along the activity axis, cathemeral (β = +0.90, [+0.73, +1.07]) and crepuscular (β = +0.48, [+0.30, +0.66]) species were significantly more likely to be absent from otherwise suitable reserves, whereas diurnal (β = −0.54, [−0.80, −0.29]) and nocturnal (β = −0.84, [−1.02, −0.64]) species were significantly more likely to be retained. Body mass had no significant effect after partialling other traits (95% CrI [−0.25, +0.03]).

Drivers of phylogenetic dark diversity (spatial GAM)

The backward-selected spatial GAM for log(EPD) explained 76.6% of the deviance (adj. $R^2 = 0.727$; Fig. 6). Five non-linear environmental terms and a strong residual spatial smoother retained statistical significance: elevation (edf = 2.53, $P < 0.001$), elevational range (edf = 1.00, $P = 0.017$), annual precipitation (edf = 2.72, $P < 0.001$), NPP (edf = 2.74, $P < 0.001$), and log-transformed sampling effort (edf = 1.92, $P = 0.017$), together with s(longitude, latitude) (edf = 17.4, $P < 0.001$). Partial-effect curves indicated that log(EPD) increased monotonically with elevational range, rose in a saturating manner with precipitation (steep through low-to-moderate rainfall, plateauing above the mean), and showed a U-shaped response to NPP (declining through intermediate productivity before rising strongly at the highest values); sampling effort had a comparatively weak, mildly non-linear effect. The standardized effect size (SES_EPD) retained only the residual spatial smoother as a significant term (edf = 17.0, $P < 0.001$), showing that the *directionality* of phylogenetic non-randomness is structured biogeographically rather than aligned with any single measured environmental gradient.

Drivers of functional dark diversity (spatial GAM)

The backward-selected GAM for log(FDI) explained 30.0% of the deviance (adj. $R^2 = 0.249$; Fig. 7a). Only two terms survived: s(logTRAPDAY) (edf = 1.00, $P = 0.003$) and s(longitude, latitude) (edf = 12.2, $P < 0.001$). No measured environmental covariate — including gHM, NPP, elevation, precipitation, elevational range or reserve age — retained significance in the final model.

Functional dispersion of the dark assemblage (FDis_dark) provided a complementary structural view (Fig. 7b–e). In its unstandardized form, FDis_dark was significantly shaped by NPP (edf = 1.00, $P = 0.020$, negative) and by residual spatial structure (edf = 9.65, $P = 0.040$). Standardized against 999 richness-preserving permutations, SES_FDis retained a negative effect of elevational range (edf = 1.00, $P = 0.031$), a negative effect of NPP (edf = 1.00, $P = 0.013$) and a marginally negative effect of sampling effort (edf = 2.59, $P = 0.079$), with no significant residual spatial smoother ($P = 0.78$) and modest overall fit (adj. $R^2 = 0.095$). The contrast between the strongly spatial log(FDI) model and the largely spatial-free SES_FDis model indicates that (i) the raw trait deficit is dominated by region-scale legacy structure, whereas (ii) once functional dispersion is standardized against richness, only two intrinsic ecological correlates — topographic heterogeneity (negative) and productivity (negative) — retain signal, consistent with a dispersion-narrowing role of physical complexity, whereby rugged terrain preserves trait extremes of the regional pool so that the residual absences are functionally similar rather than dispersion-inflating, jointly with a redundancy-driven contraction in the most productive reserves.

Regional non-randomness across biogeographic zones

The regional null-model analysis revealed a congruent north–south biogeographic gradient across the three dimensions (Fig. 4). For taxonomic dark diversity (DD_{adj}), South China carried significantly more absent species than the null expectation (SES = +4.61, FDR-$P < 0.001$), while Northeast China (SES = −4.67, FDR-$P < 0.001$), Qinghai-Tibet (SES = −3.72, FDR-$P = 0.002$) and North China (SES = −3.24, FDR-$P = 0.005$) hosted significantly fewer absent species than expected; Central China trended positively but did not reach FDR significance (SES = +2.08, FDR-$P = 0.052$). For phylogenetic dark diversity (EPD), South China (SES = +4.14, FDR-$P < 0.001$) and Southwest China (SES = +3.41, FDR-$P < 0.001$) significantly exceeded the null, while North China (SES = −6.61, FDR-$P < 0.001$), Northeast China (SES = −4.42, FDR-$P < 0.001$) and Qinghai-Tibet (SES

= −2.39, FDR-P = 0.029) fell significantly below. For functional dark diversity (FDI), South China alone significantly exceeded the null (SES = +4.13, FDR-P = 0.001), with all other regions showing non-significant deviations.

Discussion

The Anthropocene is defined by a pervasive decline in multifaceted diversity, threatening both ecosystem functioning and human well-being[3]. While protected areas (PAs) serve as the cornerstone of global conservation [5], effective spatial planning requires accounting for hidden species losses across multiple biodiversity dimensions [14]. By synthesizing the national camera-trap data with three complementary dark-diversity facets and an explicit biogeographic null-model test, our study reveals widespread, previously unmapped conservation gaps across China's PA network. Mapping these expected phylogenetic and functional absence highlights specific reserves where evolutionary history and critical ecological roles (such as key foraging guilds or body-mass classes) are disproportionately eroded relative to taxonomic richness alone. By uncovering how landscape structure and anthropogenic pressures interact to drive these hidden deficits, this national-scale assessment offers a critical, data-driven baseline for spatial conservation planning, guiding targeted rewilding efforts, habitat restoration, and the future expansion of China's reserve network to safeguard multidimensional biodiversity.

Pervasive defaunation across China's PA network

Our results reveal pervasive mammal defaunation across China's protected area network (Figure 2), with reserves retaining only a fraction of their potential mammal diversity. The high mean adjusted taxonomic dark diversity (DD_{adj} = 0.56) indicates that, on average, more than half of the ecologically suitable medium- and large-sized mammal species are absent from individual reserves, suggesting widespread community incompleteness even within areas designated for biodiversity conservation [37]. This extensive deficit suggests that protected areas have not fully preserved the

458 mammal assemblages predicted by their environmental conditions and regional species pools.
459 Instead, many reserves represent depauperate remnants of historically richer communities,
460 reflecting the long-term impacts of habitat loss, landscape fragmentation, exploitation, and other
461 anthropogenic pressures [66,67]. Importantly, the widespread occurrence of high dark diversity across
462 reserves indicates that defaunation is not confined to a small number of highly disturbed sites but
463 represents a systematic challenge for China's protected area network.
464
465 The spatial distribution of dark diversity further reveals strong geographic variation in the severity
466 of mammal community incompleteness. The highest taxonomic deficits occurred in southern China,
467 including the southern hill country, the southern margin of the Hengduan Mountains, and
468 southeastern coastal regions (Figure 4). These areas coincide with global and national hotspots of
469 mammal diversity, where species pools are exceptionally rich but where historical and
470 contemporary human pressures have also been intense [66,68]. Consequently, the high dark diversity
471 observed in these regions likely reflects the loss of species from landscapes that retain substantial
472 ecological capacity to support them. In contrast, lower dark diversity on the Qinghai–Tibet Plateau
473 and in parts of northern and northeastern China may partly reflect smaller regional species pools
474 and different biogeographic histories rather than universally intact mammal communities [47]. These
475 patterns highlight that the effectiveness of protected areas should not be evaluated solely by the
476 diversity currently present, but also by the amount of biodiversity that has been lost or remains
477 unrealized.
478
479 Beyond species-level losses, our results reveal that defaunation has also eroded evolutionary and
480 functional components of mammal diversity (Figure 2). Expected phylogenetic dark diversity
481 averaged 468 million years of missing evolutionary history, indicating that many reserves lack
482 substantial portions of the evolutionary lineages expected under their ecological conditions.
483 Similarly, the average functional deficit index of 0.22 demonstrates that protected areas also fail to

retain a considerable proportion of potential functional trait space. The broad spatial agreement among taxonomic, phylogenetic, and functional dark diversity indicates that mammal losses are not random with respect to evolutionary history or ecological roles. Instead, species absences have resulted in the disproportionate loss of particular lineages and functional strategies, potentially reducing ecosystem resilience and impairing ecological processes supported by large mammals, such as seed dispersal, herbivory, predation, and trophic regulation [69].

Nevertheless, the differences among the three dimensions of dark diversity provide important insights into the complexity of defaunation. Although taxonomic, phylogenetic, and functional deficits were positively correlated (Figure 5), their relationships were far from redundant, demonstrating that each metric captures distinct aspects of community incompleteness [70]. Species richness was strongly negatively associated with taxonomic and functional dark diversity, suggesting that reserves with fewer observed species generally experience greater deficits in species composition and ecological functions. However, phylogenetic dark diversity was independent of observed species richness, highlighting that species counts alone cannot reveal the extent of evolutionary incompleteness [71]. Integrating taxonomic, phylogenetic, and functional dark diversity therefore provides a more comprehensive assessment of hidden conservation deficits by identifying where missing species represent broader losses of evolutionary heritage and ecosystem functions. This multidimensional perspective can help prioritize restoration efforts, including habitat recovery, connectivity enhancement, and species reestablishment, thereby shifting conservation from merely preventing further losses toward restoring incomplete mammal communities [70].

Three dimensions, three driver classes

Our results demonstrate that the three dimensions of dark diversity capture complementary but non-equivalent aspects of mammal community incompleteness across China's protected-area network. Taxonomic dark diversity was primarily associated with contemporary reserve characteristics,

phylogenetic dark diversity reflected deep-time biogeographic and environmental legacy, whereas functional dark diversity represented a spatially structured historical signal that was not explained by contemporary human-pressure indices alone (Figure 3a). These results support our hypothesis that different dimensions of biodiversity loss are regulated by distinct ecological filters operating across different temporal and spatial scales. Consequently, reserve rankings differed substantially among dimensions, indicating that single-axis assessments based only on species richness or taxonomic deficits would underestimate the hidden conservation debt within protected areas [72].

Taxonomic dark diversity was mainly driven by reserve area, sampling effort and governance level (Figure 3). Larger reserves likely reduce community incompleteness by buffering wide-ranging mammals against habitat fragmentation [73], whereas increased sampling effort reduces uncertainty in estimating the observed–potential species gap [15]. The influence of governance further suggests that administrative and management contexts contribute to persistent differences in community realization among reserves [37]. Together, these findings highlight that species-level completeness remains strongly shaped by contemporary reserve conditions.

In contrast, phylogenetic dark diversity exhibited a strong environmental and historical signature (Figure 6). Mountainous and humid regions, particularly in southern and southwestern China, support deep regional phylogenetic pools because long-term climatic stability and habitat heterogeneity have facilitated lineage persistence and diversification [57,68,74]. However, many reserves within these regions currently realize only part of this evolutionary potential, resulting in substantial hidden losses of evolutionary history. Functional dark diversity showed a different pattern (Figure 7). The dependence of functional deficits on elevation range and productivity further suggests that functional dark diversity is embedded within regional ecological constraints, reflecting the interaction between historical species loss and the available functional niche space [53,75]. Together, these results emphasize that functional, phylogenetic, and taxonomic dark diversity

represent different facets of biodiversity erosion and should be integrated for comprehensive conservation assessment [70,71].

Non-random, trait-selective filtering: converging biogeographic and species-level evidence

Our results further demonstrate that mammal community incompleteness across China's protected areas is not random but strongly trait-selective. Species missing from reserves disproportionately share characteristics associated with vulnerability to anthropogenic disturbance, including threatened conservation status, dietary specialization, and activity patterns overlapping with human activity (Figure 3b). This finding places China's mammal defaunation within a broader global pattern whereby extinction risk is concentrated among species with restricted ecological strategies rather than distributed randomly across communities [39,41,42].

Threatened species were substantially over-represented in the dark pool, indicating that formal protection alone has not prevented the continued decline of vulnerable mammals. Habitat degradation around reserve boundaries, illegal hunting, and demographic limitations of small populations likely continue to restrict the persistence of species already recognized as globally threatened [42,43]. Dietary specialization further increased the likelihood of absence: strict herbivores and carnivores were more frequently missing, whereas omnivores were preferentially retained. This pattern likely reflects the greater ecological constraints faced by specialists, which have fewer alternatives when food resources decline or landscapes become fragmented [40,42].

Activity pattern also emerged as an important persistence filter. Species whose activity overlaps with human daytime activity, particularly cathemeral and crepuscular mammals, were more likely to be absent, whereas strictly nocturnal or diurnal species were better represented. This suggests that temporal avoidance of human disturbance may facilitate persistence in human-dominated landscapes [76]. Together, these trait-level patterns reveal a coherent syndrome of vulnerability,

identifying the types of mammals most likely to contribute to hidden biodiversity deficits within protected areas.

Conservation implications of multidimensional dark diversity

Integrating multidimensional dark diversity into protected-area evaluation provides a shift from assessing only "what remains" toward identifying "what should be present but is missing." [37] This perspective is particularly important for China's protected-area network, where many reserves retain substantial ecological potential but currently support incomplete mammal assemblages [19]. High dark diversity, especially when detected simultaneously across taxonomic, phylogenetic, and functional dimensions, represents a hidden conservation debt and a priority for restoration rather than evidence of conservation success [77]. Our results suggest several practical implications. First, reserves in southern China with consistently elevated dark diversity should be prioritized for active restoration, including habitat recovery, landscape connectivity enhancement, prey-base restoration, and improved protection against hunting. Second, phylogenetic and functional dark diversity provide essential information beyond species counts by identifying reserves that have lost disproportionate amounts of evolutionary history or ecological roles despite maintaining relatively high richness [17,78]. Third, restoration efforts should target trait groups most associated with hidden absence, including threatened specialists, large herbivores, carnivores, and species sensitive to human disturbance [79]. Finally, standardized camera-trap monitoring combined with dark-diversity metrics can transform biodiversity surveys from inventories of existing species into proactive assessments of recovery potential. By revealing the missing components of mammal communities, multidimensional dark diversity provides a forward-looking framework for conservation planning. Rather than simply expanding protected areas or preventing additional losses, conservation strategies should aim to restore ecological integrity by recovering the evolutionary lineages, functional roles, and species assemblages that protected areas were originally established to conserve.

Conclusions

Across 199 terrestrial nature reserves in China, medium- and large-sized mammal communities are missing, on average, more than half of the species expected under their ecological conditions, revealing pervasive and non-random defaunation within the protected-area network. This community incompleteness extends beyond species loss to the erosion of evolutionary history and functional potential, with taxonomic, phylogenetic, and functional dark diversity reflecting distinct but complementary ecological filters. By integrating multidimensional dark diversity with biogeographic null models, protected-area assessments can move beyond measuring what remains to reveal what is missing and potentially recoverable, providing a powerful framework for prioritizing restoration, connectivity enhancement, and species-recovery actions under global biodiversity goals.

Acknowledgements

We are indebted to the hundreds of field teams whose primary camera-trap studies, published between 2010 and 2025, formed the empirical backbone of this synthesis; without their long-term commitment to standardized monitoring across China's reserve network, a national-scale dark-diversity study would not have been possible. We thank Madis Pärtel, Carlos P. Carmona, and Jun Fujinuma for clarifying methodological aspects of the dark-diversity, expected phylogenetic dark diversity and species–site unified frameworks, respectively. The research group acknowledges supports from the the National Natural Science Foundation of China (#32370562), and the China Biodiversity Monitoring and Research Network (Sino BON).

Competing Interests

The authors declare no competing financial or non-financial interests.

Ethics declarations

The study is based exclusively on previously published, peer-reviewed camera-trap datasets and on publicly available environmental, phylogenetic and trait databases. All primary data sources are cited in the Supplementary Material.

Data Availability

The data and R scripts produced all the results and figures for this study can be accessed in figshare through the following private link: https://figshare.com/s/296aeb6fea7837d6287e. This resource will be made publicly available from the date of publication of this manuscript.

References

1. Oliver, R. Y. *et al.* Interacting effects of human presence and landscape modification on birds and mammals. *Science* **392**, 879–884 (2026).
2. Keck, F. *et al.* The global human impact on biodiversity. *Nature* **641**, 395–400 (2025).
3. Liu, Y., Onditi, K. O., Hu, W., Jiang, X. & Li, X. Human Pressures Drive Compositional Homogenization and Functional Shifts in Southeast Asian Mammal Communities. *Glob. Change Biol.* **32**, e70916 (2026).
4. Geldmann, J., Jones, J. P. G., Wauchope, H. & Ferraro, P. J. Causal claims, causal assumptions and protected area impact. *Nature* **638**, E40–E41 (2025).
5. Brodie, J. F. *et al.* Landscape-scale benefits of protected areas for tropical biodiversity. *Nature* **620**, 807–812 (2023).
6. *CBD (Convention on Biological Diversity). The Kunming-Montreal Global Biodiversity Framework. Https://Www.Cbd.Int/Doc/Decisions/Cop-15/Cop-15-Dec-04-En.Pdf.* (2022).
7. Li, X. *et al.* Functional homogenization of terrestrial mammals outside protected areas in the Hengduan Mountains, China. *Conserv. Biol.* **40**, e70214 (2026).
8. Orme, C. D. L. *et al.* Global hotspots of species richness are not congruent with endemism or threat. *Nature* **436**, 1016–1019 (2005).
9. Li, X. *et al.* Beyond species richness: habitat fragmentation reduces community occupancy and functional richness of mountain forest mammals. *Biol. Conserv.* **318**, 111828 (2026).

10. Pärtel, M., Szava-Kovats, R. & Zobel, M. Dark diversity: shedding light on absent species. *Trends Ecol. Evol.* **26**, 124–128 (2011).
11. Gavriel, T. *et al.* Using dark diversity to disentangle the effects of protection and habitat quality on species diversity. *Biol. Conserv.* **305**, 111096 (2025).
12. Fernandes, C. S., Batalha, M. A. & Bichuette, M. E. Dark diversity in the dark: a new approach to subterranean conservation. *Subterr. Biol.* **32**, 69–80 (2019).
13. Riibak, K. *et al.* Dark diversity in dry calcareous grasslands is determined by dispersal ability and stress-tolerance. *Ecography* **38**, 713–721 (2015).
14. Lewis, R. J. *et al.* Applying the dark diversity concept to nature conservation. *Conserv. Biol.* **31**, 40–47 (2017).
15. Fujinuma, J. & Pärtel, M. Decomposing dark diversity affinities of species and sites using Bayesian method: what accounts for absences of species at suitable sites? *Methods Ecol. Evol.* **14**, 1796–1807 (2023).
16. Wan, J. Z. & Wang, X. Environmental heterogeneity drives the dark diversity of global plant communities. *J. Biogeogr.* **52**, e70043 (2025).
17. Morel, L., Jung, V., Chollet, S., Ysnel, F. & Barbe, L. From taxonomic to functional dark diversity: Exploring the causes of potential biodiversity and its implications for conservation. *J. Appl. Ecol.* **59**, 103–116 (2022).
18. Wen, Z. *et al.* Using completeness and defaunation indices to understand nature reserve's key attributes in preserving medium- and large-bodied mammals. *Biol. Conserv.* **241**, 108273 (2020).

19. Zhang, L. *et al.* Conservation effectiveness of Chinese protected areas on the completeness of medium- and large-bodied mammal community. *Biol. Conserv.* **306**, 111128 (2025).
20. Faith, D. P. Phylogenetic diversity, functional trait diversity and extinction: avoiding tipping points and worst-case losses. *Philos. Trans. R. Soc. B Biol. Sci.* **370**, 20140011 (2015).
21. Werneck, R. P., Sobral, F. L. & Cianciaruso, M. V. Protected areas with high species, phylogenetic, and functional diversity are complementary and occur in heavily modified Cerrado landscapes. *J. Nat. Conserv.* **90**, 127204 (2026).
22. Bogoni, J. A., Ferraz, K. M. P. M. B. & Peres, C. A. Continental-scale local extinctions in mammal assemblages are synergistically induced by habitat loss and hunting pressure. *Biol. Conserv.* **272**, 109635 (2022).
23. Galetti, M. *et al.* Ecological and evolutionary legacy of megafauna extinctions. *Biol. Rev.* **93**, 845–862 (2018).
24. Ripple, W. J. *et al.* Status and ecological effects of the world's largest carnivores. *Science* **343**, 1241484 (2014).
25. Kuussaari, M. *et al.* Extinction debt: a challenge for biodiversity conservation. *Trends Ecol. Evol.* **24**, 564–571 (2009).
26. Zhang, W.-G. *et al.* Dark diversity framework reconciles Darwin's naturalization conundrum for freshwater fish invasions. *Proc. Natl. Acad. Sci.* **123**, e2604929123 (2026).

27. Panter, C. T. *et al.* Plants with higher dispersal capabilities follow 'abundant-centre' distributions but such patterns remain rare in animals. *Nat. Commun.* **16**, 8205 (2025).
28. Trindade, D. P. F., Carmona, C. P. & Pärtel, M. Temporal lags in observed and dark diversity in the Anthropocene. *Glob. Change Biol.* **26**, 3193–3201 (2020).
29. Tucker, M. A. *et al.* Moving in the Anthropocene: Global reductions in terrestrial mammalian movements. *Science* **359**, 466–469 (2018).
30. Greco, I. *et al.* Placement matters: implications of trail- versus random-based camera-trap deployment for monitoring mammal communities. *Ecol. Appl.* **35**, e70083 (2025).
31. Silva-Rodríguez, E. A. *et al.* A protocol for error prevention and quality control in camera trap datasets. *J. Appl. Ecol.* **62**, 773–782 (2025).
32. Steenweg, R. *et al.* Scaling-up camera traps: monitoring the planet's biodiversity with networks of remote sensors. *Front. Ecol. Environ.* **15**, 26–34 (2017).
33. Krasnov, B. R., Vinarski, M. V., Korallo-Vinarskaya, N. P., Khokhlova, I. S. & Grabovsky, V. I. Parasite traits, host traits, and environment as determinants of dark diversity affinity in flea and gamasid mite assemblages from the Palearctic. *Parasitol. Res.* **123**, 396 (2024).
34. Pärtel, M. *et al.* Global impoverishment of natural vegetation revealed by dark diversity. *Nature* **641**, 917–924 (2025).
35. Jiang, Z., Wu, Y., Liu, S. & Jiang, X. *China's Mammal Diversity*. (Science Press, Beijing, 2017).

36. Zhu, S., Tian, J., Yue, J., Duan, F. & Li, S. Updating the Species Inventory of Large- and Medium-Sized Mammals in China Based on 2009–2020 Field Observation Records. *Animals* **14**, 3380 (2024).
37. Xu, W. *et al.* Transforming protected area management in China. *Trends Ecol. Evol.* **34**, 762–766 (2019).
38. Yang, H., Huang, Q., Zhang, J., Songer, M. & Liu, J. Range-wide assessment of the impact of China's nature reserves on giant panda habitat quality. *Sci. Total Environ.* **769**, 145081 (2021).
39. Dirzo, R. *et al.* Defaunation in the Anthropocene. *Science* **345**, 401–406 (2014).
40. Ripple, W. J. *et al.* Collapse of the world's largest herbivores. *Sci. Adv.* **1**, e1400103 (2015).
41. Cardillo, M. *et al.* Multiple causes of high extinction risk in large mammal species. *Science* **309**, 1239–1241 (2005).
42. Cooke, R. S. C., Eigenbrod, F. & Bates, A. E. Projected losses of global mammal and bird ecological strategies. *Nat. Commun.* **10**, 2279 (2019).
43. Toussaint, A. *et al.* Extinction of threatened vertebrates will lead to idiosyncratic changes in functional diversity across the world. *Nat. Commun.* **12**, 5162 (2021).
44. Zhao, F. *et al.* Comparing elevational patterns of taxonomic, phylogenetic, and functional diversity of woody plants reveal the asymmetry of community assembly mechanisms on a mountain in the hengduan mountains region. *Front. Ecol. Evol.* **10**, 869258 (2022).
45. Zu, K. *et al.* Latitudinal gradients of angiosperm plant diversity and phylogenetic structure in China's nature reserves. *Glob. Ecol. Conserv.* **42**, e02403 (2023).

46. Myers, N., Mittermeier, R. A., Mittermeier, C. G., da Fonseca, G. A. B. & Kent, J. Biodiversity hotspots for conservation priorities. *Nature* **403**, 853–858 (2000).
47. Zhang R.-Z. *Zoogeography of China*. (Science Press, Beijing, 2011).
48. Tobler, M. W., Carrillo-Percastegui, S. E., Leite Pitman, R., Mares, R. & Powell, G. An evaluation of camera traps for inventorying large- and medium-sized terrestrial rainforest mammals. *Anim. Conserv.* **11**, 169–178 (2008).
49. Jiang, Z. *et al.* Red list of China's vertebrates. *Biodivers. Sci.* **24**, 500 (2016).
50. Bruelheide, H., Jiménez-Alfaro, B., Jandt, U. & Sabatini, F. M. Deriving site-specific species pools from large databases. *Ecography* **43**, 1215–1228 (2020).
51. Lewis, R. J., Szava-Kovats, R. & Pärtel, M. Estimating dark diversity and species pools: an empirical assessment of two methods. *Methods Ecol. Evol.* **7**, 104–113 (2016).
52. Jung, M. *et al.* A global map of terrestrial habitat types. *Sci. Data* **7**, 256 (2020).
53. Liu, J., Kang, Y., Kays, R., Jensen, A. J. & Jiang, A. Apex predator loss drives trophic downgrading in China's protected areas. *Curr. Biol.* **35**, 2989-2997.e3 (2025).
54. Carmona, C. P. & Pärtel, M. Estimating probabilistic site-specific species pools and dark diversity from co-occurrence data. *Glob. Ecol. Biogeogr.* **30**, 316–326 (2021).
55. Paganeli, B., Fujinuma, J., Trindade, D. P. F., Carmona, C. P. & Pärtel, M. A roadmap to carefully select methods for dark-diversity studies. *J. Veg. Sci.* **35**, e13264 (2024).
56. Hu, Y. *et al.* Functional and phylogenetic structure of mammals along elevational gradients in the Central and East Himalayas. *Ecol. Process.* **13**, 65 (2024).

57. Qian, H., Qian, S., Zhang, J. & Kessler, M. Effects of climate and environmental heterogeneity on the phylogenetic structure of regional angiosperm floras worldwide. *Nat. Commun.* **15**, 1079 (2024).
58. Wright, D. H. Species-Energy Theory: An Extension of Species-Area Theory. *Oikos* **41**, 496–506 (1983).
59. Moeslund, J. E. *et al.* Using dark diversity and plant characteristics to guide conservation and restoration. *J. Appl. Ecol.* **54**, 1730–1741 (2017).
60. Valdez, J. W. *et al.* Relationships between macro-fungal dark diversity and habitat parameters using LiDAR. *Fungal Ecol.* **51**, 101054 (2021).
61. Upham, N. S., Esselstyn, J. A. & Jetz, W. Inferring the mammal tree: Species-level sets of phylogenies for questions in ecology, evolution, and conservation. *PLOS Biol.* **17**, e3000494 (2019).
62. Wilman, H. *et al.* EltonTraits 1.0: Species-level foraging attributes of the world's birds and mammals: Ecological Archives E095-178. *Ecology* **95**, 2027–2027 (2014).
63. Ding, C. *et al.* A dataset on the morphological, life-history and ecological traits of the mammals in China. *Biodivers. Sci.* **30**, 21520 (2022).
64. Atwood, T. B. *et al.* Herbivores at the highest risk of extinction among mammals, birds, and reptiles. *Sci. Adv.* **6**, eabb8458 (2020).
65. Plummer, M. rjags: Bayesian Graphical Models using MCMC. CRAN (2024).
66. Liu, J., Kang, Y., Kays, R., Jensen, A. J. & Jiang, A. Apex predator loss drives trophic downgrading in China's protected areas. *Curr. Biol.* **35**, 2989-2997.e3 (2025).
67. He, J. *et al.* Widespread range contraction of carnivores in protected areas of China. *Nat. Sustain.* 1–10 (2026) doi:10.1038/s41893-026-01855-2.

68. Hu, Y. *et al.* Spatial patterns and conservation of genetic and phylogenetic diversity of wildlife in China. *Sci. Adv.* **7**, eabd5725 (2021).
69. Bogoni, J. A., Peres, C. A. & Ferraz, K. M. P. M. B. Effects of mammal defaunation on natural ecosystem services and human well being throughout the entire Neotropical realm. *Ecosyst. Serv.* **45**, 101173 (2020).
70. Liu, Y., Wang, J., Wu, Z., Xu, Z. & Abulike, K. Integrating multidimensional biodiversity into spatial conservation planning to bridge conservation gaps in China. *Biol. Conserv.* **314**, 111664 (2026).
71. Devictor, V. *et al.* Spatial mismatch and congruence between taxonomic, phylogenetic and functional diversity: the need for integrative conservation strategies in a changing world. *Ecol. Lett.* **13**, 1030–1040 (2010).
72. Pires, M. M. & Galetti, M. Beyond the 'empty forest': The defaunation syndromes of Neotropical forests in the Anthropocene. *Glob. Ecol. Conserv.* **41**, e02362 (2023).
73. Fahrig, L. Effects of habitat fragmentation on biodiversity. *Annu. Rev. Ecol. Evol. Syst.* **34**, 487–515 (2003).
74. Robuchon, M. *et al.* Revisiting species and areas of interest for conserving global mammalian phylogenetic diversity. *Nat. Commun.* **12**, 3694 (2021).
75. Wan, X. *et al.* Historical records reveal the distinctive associations of human disturbance and extreme climate change with local extinctions of mammals. *Proc. Natl. Acad. Sci.* **116**, 19001–19008 (2019).
76. Gaynor, K. M., Hojnowski, C. E., Carter, N. H. & Brashares, J. S. The influence of human disturbance on wildlife nocturnality. *Science* **360**, 1232–1235 (2018).

77. Chollet, S., Dano, M., Thiébaut, G. & Jung, V. Dark diversity and habitat conservation status: Two sides of the same coin for conservation and restoration? *Ecol. Indic.* **170**, 112990 (2025).
78. Mazel, F. *et al.* Prioritizing phylogenetic diversity captures functional diversity unreliably. *Nat. Commun.* **9**, 2888 (2018).
79. Li, X. Y. *et al.* Functional diversity loss and change in nocturnal behavior of mammals under anthropogenic disturbance. *Conserv. Biol.* **36**, (2022).

Figure legends

Figure 1 | The Chinese terrestrial nature-reserve camera-trap network used in this study. Distribution of the 199 reserves (coloured by zoogeographic region; symbol area proportional to √reserve area) that met our inclusion criteria (>30 deployed cameras, >400 effective camera-days, complete species list). Reserves span all seven of China's zoogeographic regions and the full latitudinal, longitudinal and elevational extent of mainland China. Across the network the cumulative monitoring effort exceeded 7.4×10^6 camera-trap days and yielded independent detections of 105 medium- and large-sized mammal species.

Figure 2 | Multidimensional spatial structure of dark diversity for medium- and large-sized mammals across China. a, Adjusted taxonomic dark diversity (DD_{adj}). **b**, Expected phylogenetic dark diversity (EPD). **c**, Functional deficit index (FDI). Each dot is a reserve; warm and cool colours respectively denote high and low values. Dashed lines outline China's seven zoogeographic regions following Zhang (2011): NE, Northeast China; NC, North China; MX, Mongolian-Xinjiang; QT, Qinghai-Tibet; SW, Southwest China; CC, Central China; SC, South China. All three dimensions are highest in southern and parts of east-central China and lowest in high-altitude western and northern reserves. Observed species richness is significantly negatively correlated with the taxonomic and functional dimensions (Spearman $\rho = -0.60$ with DD_{adj}, -0.61 with FDI; both $P < 0.001$) but decoupled from the phylogenetic dimension ($\rho = -0.04$, $P = 0.62$), establishing that richness alone does not signal community completeness.

Figure 3 | Drivers of taxonomic dark-diversity affinity from the Bayesian species–site unified model. a, Site-level posterior densities for environmental, sampling, governance and zoogeographic covariates. **b**, Species-level posterior densities for traits (body mass, diet, activity, IUCN threat status). Black-filled densities indicate parameters whose 95% credible interval excludes zero (i.e. significant effects); grey densities are non-significant. The vertical solid line

marks zero. At the site level, reserve area and sampling effort and Municipal-level governance significantly reduce dark-diversity affinity; Southwest and North China have significantly positive regional intercepts, whereas South China has a significantly negative one after partialling other covariates. At the species level, IUCN-threatened status, herbivory, carnivory and cathemeral/crepuscular activity significantly increase dark-diversity affinity; omnivory, diurnal and nocturnal activity, and non-threatened status significantly decrease it.

Figure 4 | Biogeographic null-model analysis of community incompleteness across China's seven zoogeographic regions. For each dimension (**a**, taxonomic; **b**, phylogenetic; **c**, functional), the left panel shows the standardized effect size (SES) of regional mean dark diversity relative to 9999 reshuffling permutations of reserve values, with two-tailed FDR-adjusted significance indicated (*** $P < 0.001$; ** $P < 0.01$; * $P < 0.05$; ns non-significant). Bars indicate regions with significantly more absent species than expected ("higher than null", orange), significantly fewer absent species than expected ("lower than null", blue), or non-significant deviations (grey). The right panel contrasts observed regional means (coloured points) with the null expectation (black points and 95% null intervals, grey segments). South China carries significantly more absent species than expected across all three dimensions, whereas North China, Northeast China and Qinghai-Tibet show significantly fewer on the taxonomic and phylogenetic axes. The functional-dimension panel (c) has n = 198 rather than 199 because a single South-China reserve (Yunnan Dawei Shan, with only two observed species) carried insufficient trait-space information to compute FDis-based metrics; the taxonomic (a) and phylogenetic (b) panels retain the full 199-reserve dataset.

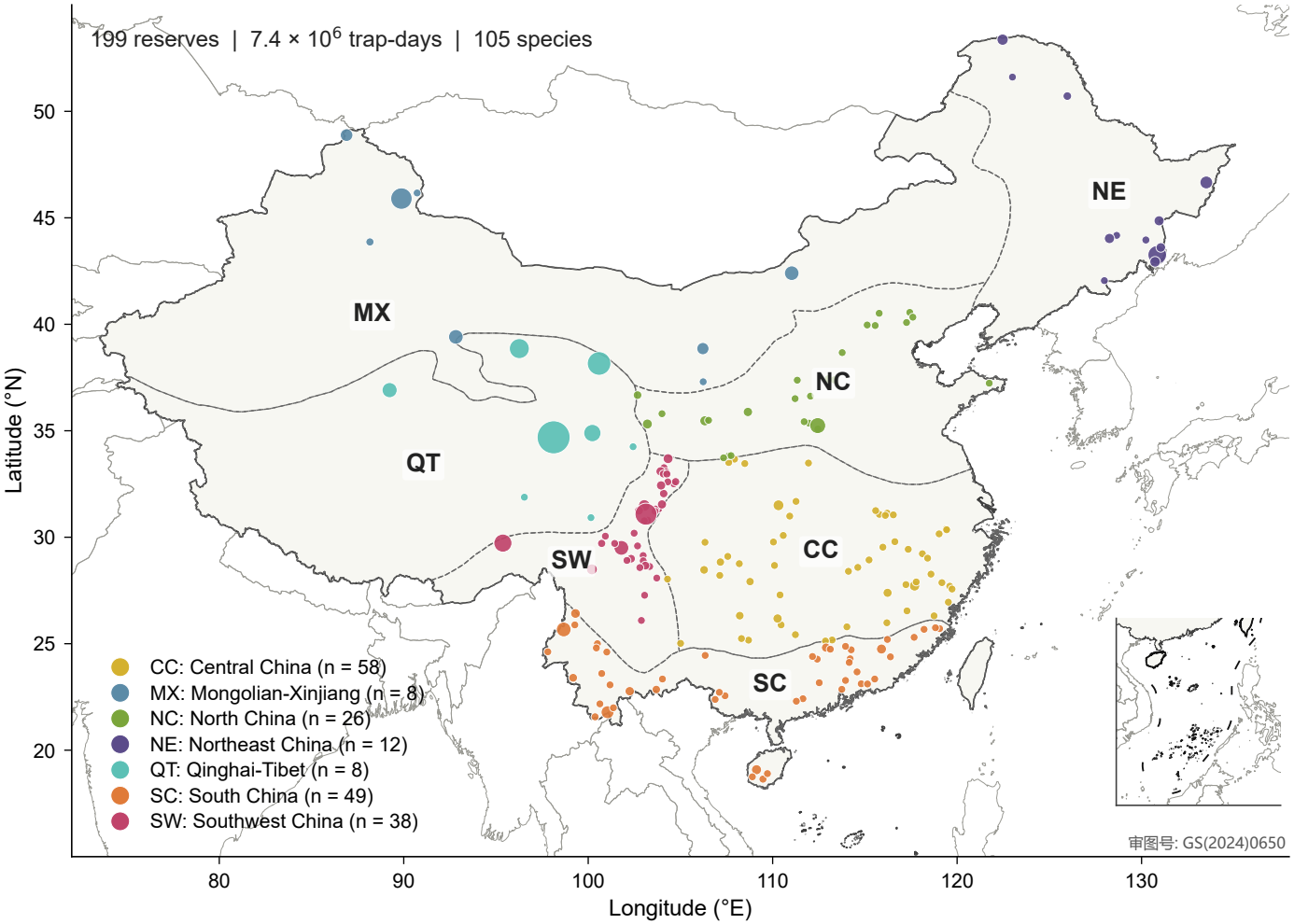
Figure 5 | Coupled but non-redundant signatures of community incompleteness. Pairwise relationships between observed species richness (SR) and the three dark-diversity dimensions across 199 reserves. Diagonal: kernel density distributions. Lower triangle: bivariate scatter plots

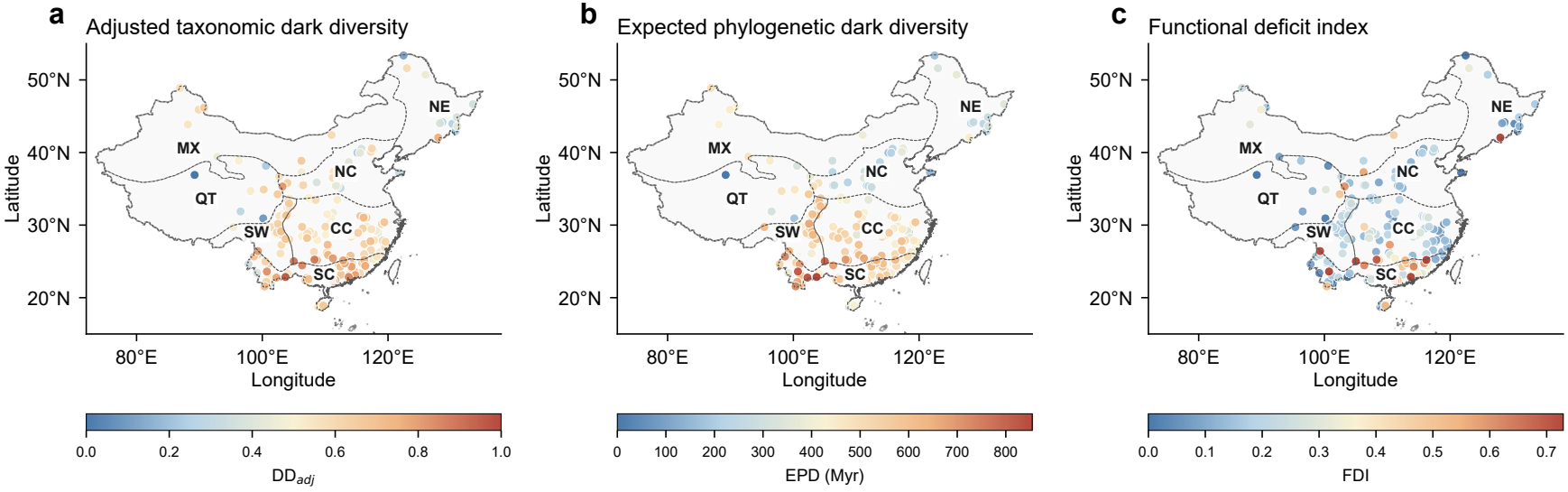
with linear fits. Upper triangle: Spearman rank correlations (rho) and significance (*** $P <$ 0.001). The taxonomic and functional dimensions are strongly negatively correlated with observed richness ($\rho = -0.60$ to -0.61); the phylogenetic dimension is decoupled from richness ($\rho = -0.04$, n.s.). The three dark-diversity dimensions are positively correlated with one another ($\rho =$ 0.44 to 0.74), but the inter-dimensional correlations are well below unity — confirming that taxonomic, phylogenetic and functional incompleteness capture overlapping but ecologically distinct facets of the conservation deficit.

Figure 6 | Environmental drivers of phylogenetic dark diversity (log-transformed expected phylogenetic dark diversity, log(EPD)). Backward-selected spatially explicit generalized additive model (Gaussian family with identity link; adj. $R^2 = 0.727$, deviance explained = 76.6%, n = 199). Panels **a**–**e** show partial effects of the five significant non-linear environmental smoothers with 95% pointwise confidence bands (shaded); grey dots are partial residuals. **a**, Elevation. **b**, Elevational range. **c**, Annual precipitation. **d**, Net primary productivity (NPP). **e**, Log-transformed camera-trap sampling effort. Effective degrees of freedom (edf) and Wald *P* values are annotated in each panel. The residual bivariate spatial smoother s(longitude, latitude) (edf = 17.4, $P < 0.001$) is omitted here for readability and is mapped in Fig. S3. Continuous environmental covariates were standardized (z-score) prior to modelling; back-transformed axis units are shown for elevation, elevational range and sampling effort.

Figure 7 | Generalized additive models for functional dark diversity. Backward-selected GAMs for three complementary functional metrics (Gaussian family with identity link). **a**, log-transformed functional deficit index, log(FDI): partial effect of camera-trap sampling effort; adj. $R^2 = 0.249$, deviance explained = 30.0%. **b**, unstandardized functional dispersion of the dark assemblage, FDis_dark: partial effect of NPP. **c**–**e**, standardized effect size for functional dispersion, SES_FDis (999 richness-preserving permutations; adj. $R^2 = 0.095$): partial effects of **c**

elevational range, **d** NPP, and **e** log-transformed sampling effort. Shaded areas are 95% pointwise confidence bands; grey dots are partial residuals. Effective degrees of freedom and Wald *P* values are annotated in each panel. The residual spatial smoother s(longitude, latitude) was significant for log(FDI) (edf = 12.2, $P < 0.001$) and FDis_dark (edf = 9.65, $P = 0.040$) but not for SES_FDis ($P = 0.78$); the two significant spatial smoothers are mapped in Fig. S5. Overall, raw functional loss is dominated by region-scale historical processes captured in residual space, whereas once dispersion is standardized against richness, only intrinsic ecological correlates — elevational range (negative) and NPP (negative) — retain signal.


199 reserves | 7.4 × 10^6 trap-days | 105 species
NE
MX
NC
QT
SW
CC
SC
CC: Central China (n = 58)
MX: Mongolian-Xinjiang (n = 8)
NC: North China (n = 26)
NE: Northeast China (n = 12)
QT: Qinghai-Tibet (n = 8)
SC: South China (n = 49)
SW: Southwest China (n = 38)
Latitude (°N)
Longitude (°E)
50
45
40
35
30
25
20
80
90
100
110
120
130
审图号: GS(2024)0650


a
Adjusted taxonomic dark diversity
b
Expected phylogenetic dark diversity
c
Functional deficit index
50°N
40°N
30°N
20°N
Latitude
80°E
100°E
120°E
Longitude
NE
MX
NC
QT
SW
CC
SC
0.0
0.2
0.4
0.6
0.8
1.0
DD$_{adj}$
0
100
200
300
400
500
600
700
800
EPD (Myr)
0.0
0.1
0.2
0.3
0.4
0.5
0.6
0.7
FDI

a **Site-level DDA regression**

95% CI < 0 | 95% CI overlaps 0 | 95% CI > 0

Environmental & sampling
- Precipitation
- Global human modification (gHM)
- Elevation range (ER)
- Landscape patch density (PD)
- Net primary productivity (NPP)
- Elevation
- Sampling effort (log-days)
- Reserve area

Zoogeographic region
- Region: Southwest China
- Region: North China
- Region: Northeast China
- Region: Mongolian-Xinjiang
- Region: Qinghai-Tibet
- Region: Central China
- Region: South China

Reserve level
- Reserve level: County
- Reserve level: National
- Reserve level: Provincial
- Reserve level: Municipal

-1.5 -1.0 -0.5 0.0 0.5 1.0 1.5

Standardized regression coefficient

b **Species-level DDA regression**

95% CI < 0 | 95% CI overlaps 0 | 95% CI > 0

Body mass
- Body mass (log-scaled)

Diet
- Diet: Herbivore
- Diet: Carnivore
- Diet: Omnivore

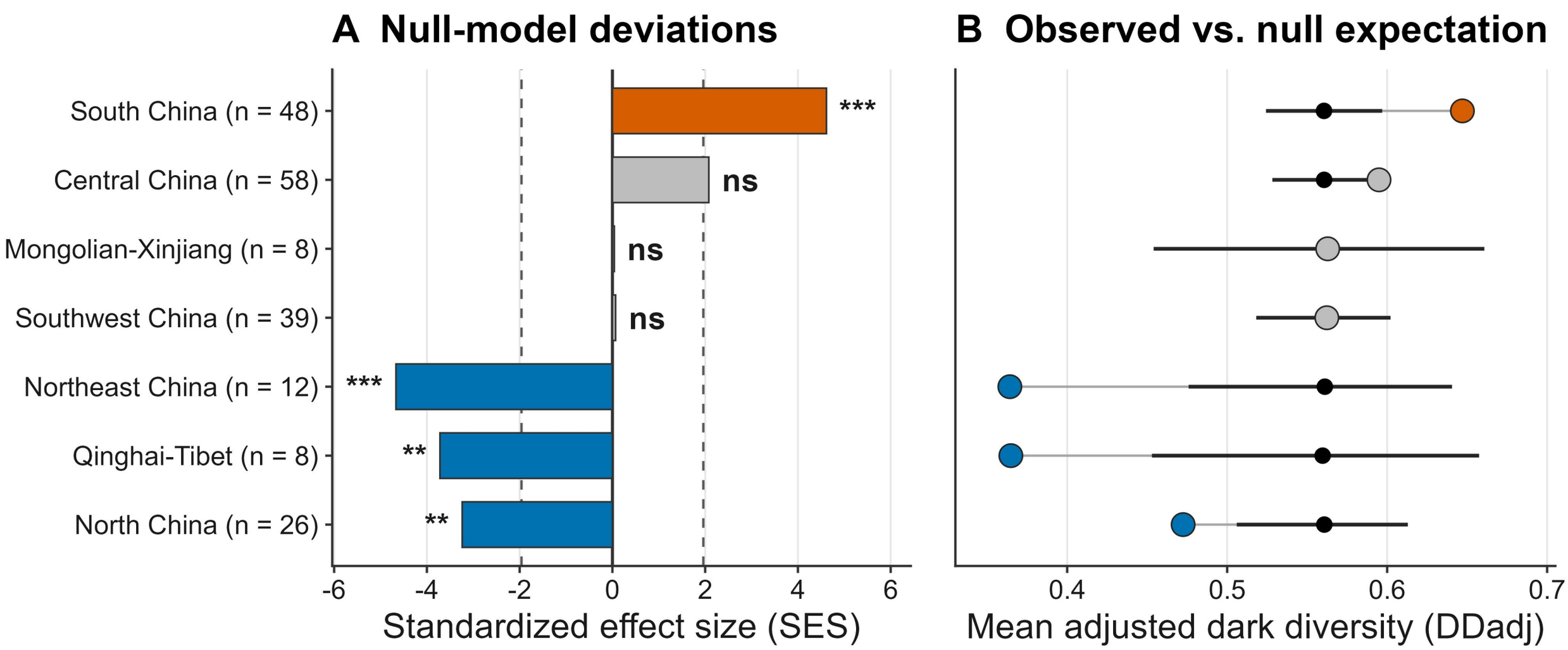
Activity
- Activity: Cathemeral
- Activity: Crepuscular
- Activity: Diurnal
- Activity: Nocturnal

IUCN status
- IUCN: Threatened
- IUCN: Non-threatened

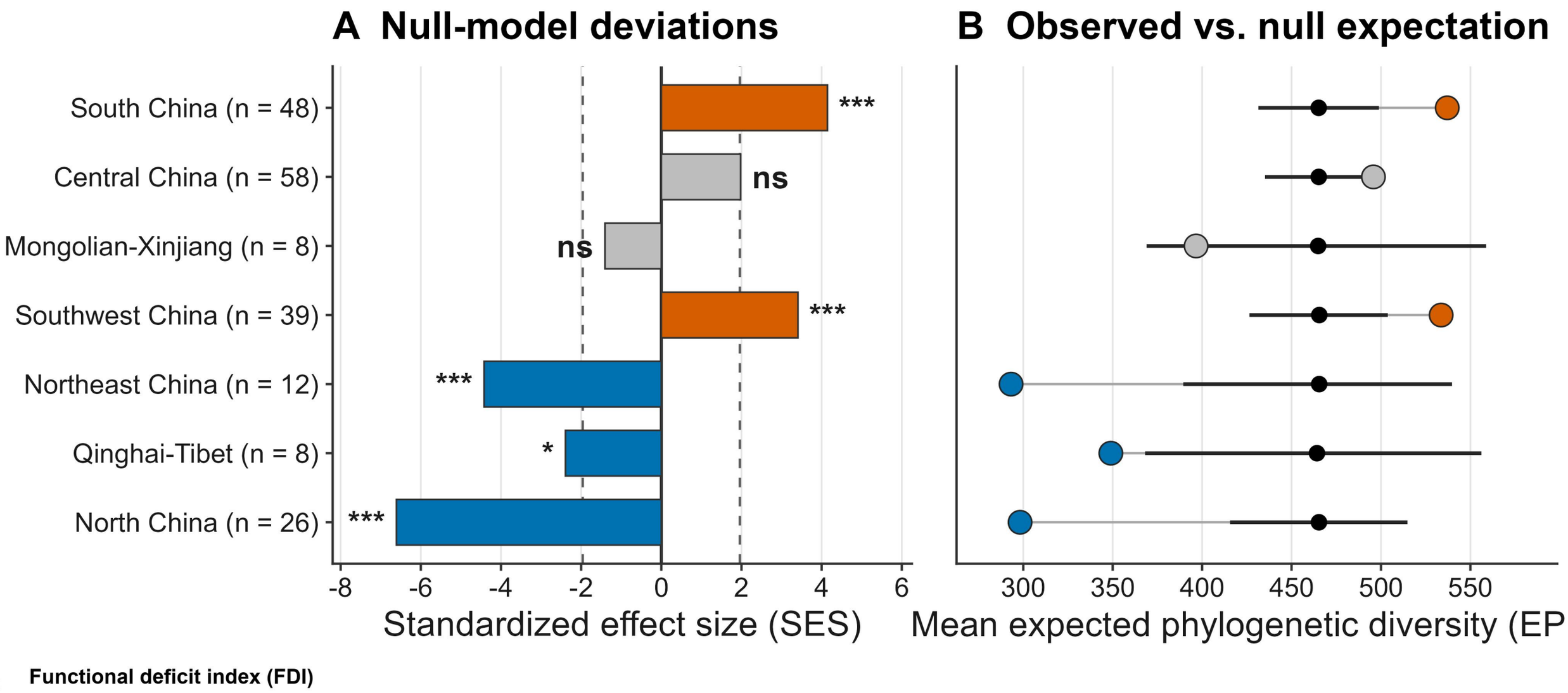
-1.5 -1.0 -0.5 0.0 0.5 1.0 1.5

Standardized regression coefficient

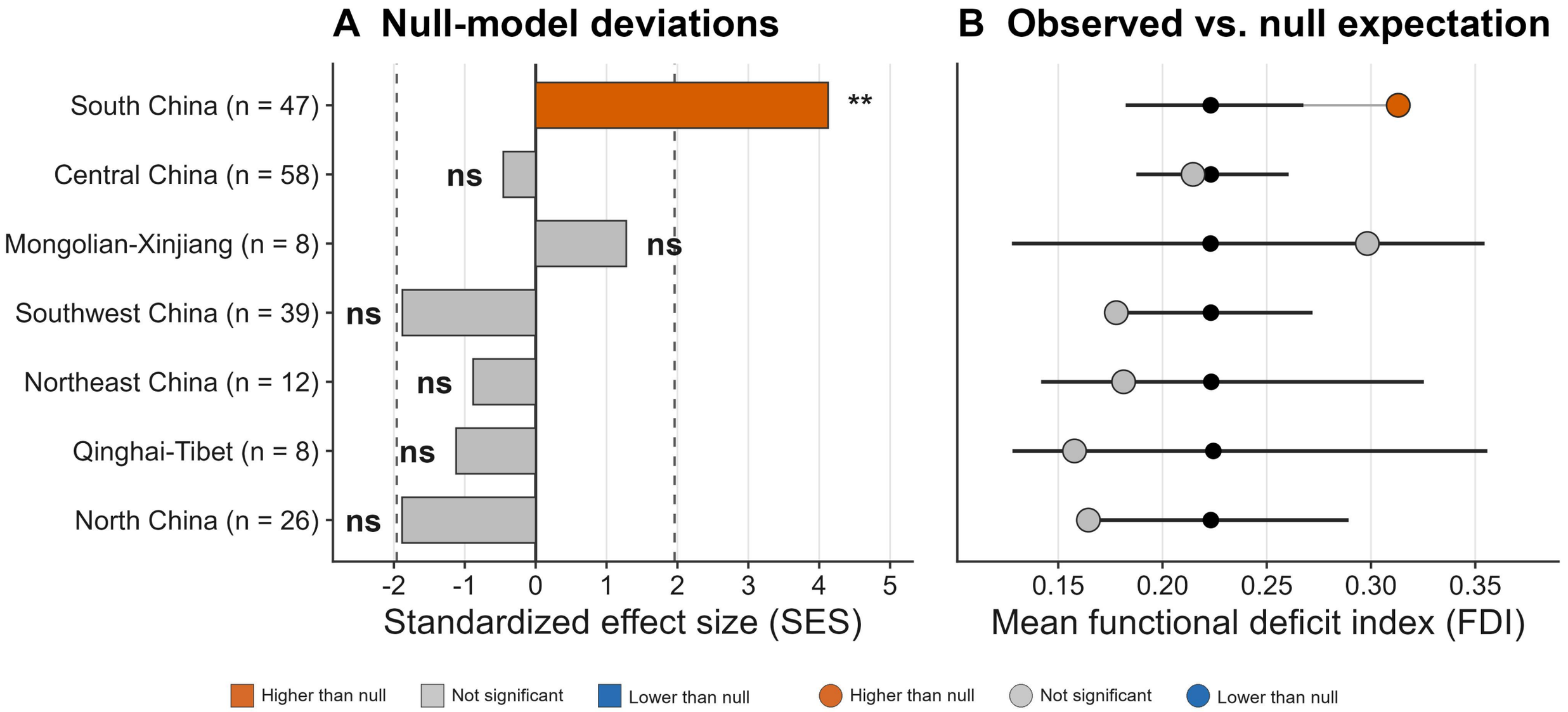
a Taxonomic dark diversity (DD_adj)

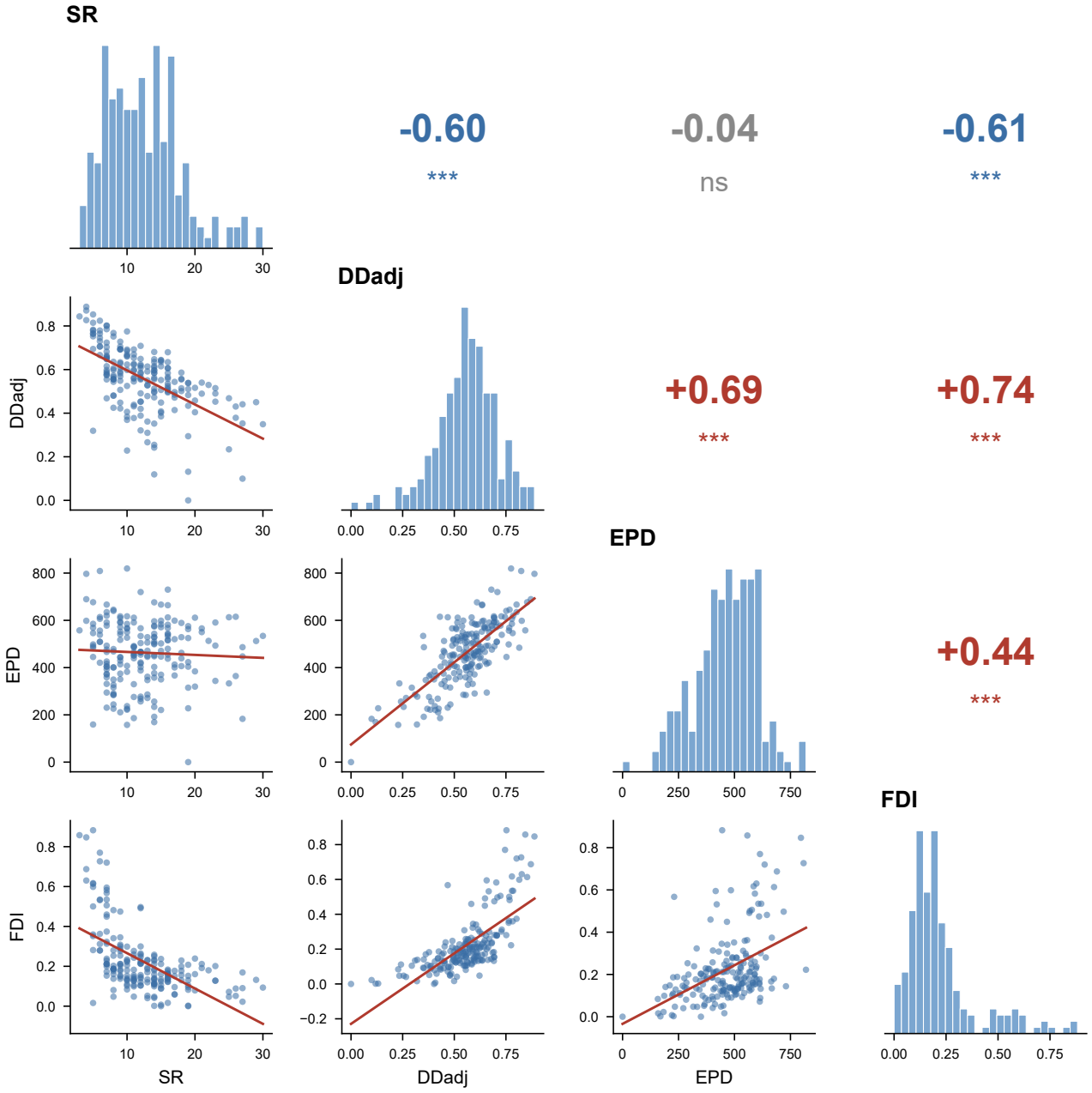


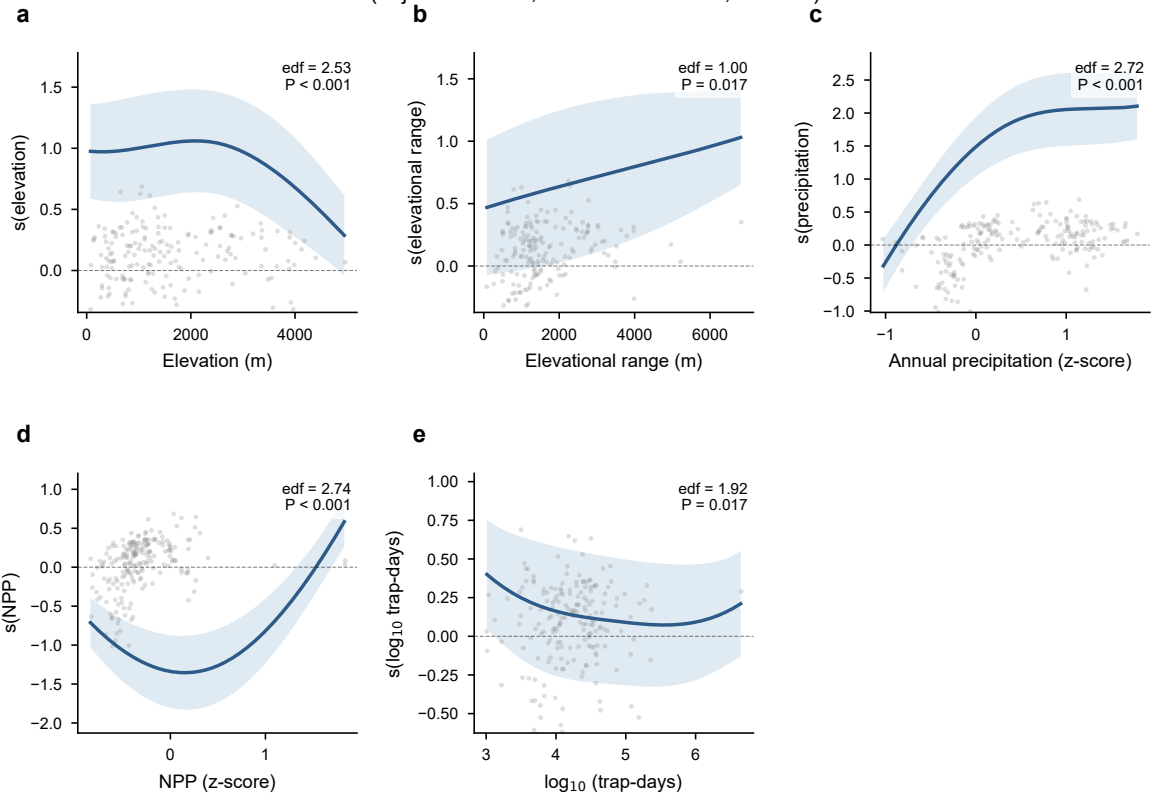
b Phylogenetic dark diversity (EPD)

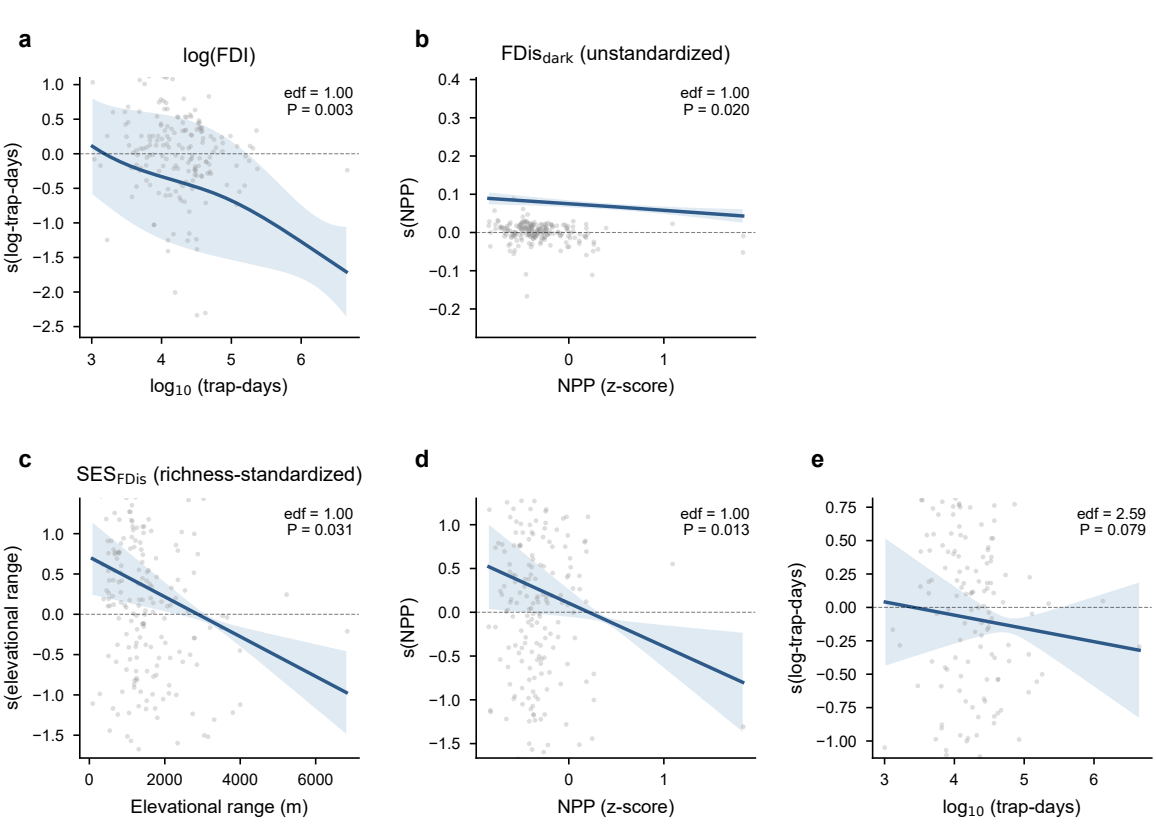


c Functional deficit index (FDI)




SR
DDadj
EPD
FDI
-0.60
***
-0.04
ns
-0.61
***
+0.69
***
+0.74
***
+0.44
***
SR
DDadj
EPD
FDI


Environmental drivers of log(EPD)
(adj. R^2 = 0.727, deviance = 76.6%, n = 199)
a
edf = 2.53
P < 0.001
s(elevation)
Elevation (m)
b
edf = 1.00
P = 0.017
s(elevational range)
Elevational range (m)
c
edf = 2.72
P < 0.001
s(precipitation)
Annual precipitation (z-score)
d
edf = 2.74
P < 0.001
s(NPP)
NPP (z-score)
e
edf = 1.92
P = 0.017
s(log10 trap-days)
log10 (trap-days)


GAMs for functional dark diversity (n = 199)
a
log(FDI)
edf = 1.00
P = 0.003
s(log-trap-days)
log10 (trap-days)
b
FDisdark (unstandardized)
edf = 1.00
P = 0.020
s(NPP)
NPP (z-score)
c
SESFDis (richness-standardized)
edf = 1.00
P = 0.031
s(elevational range)
Elevational range (m)
d
edf = 1.00
P = 0.013
s(NPP)
NPP (z-score)
e
edf = 2.59
P = 0.079
s(log-trap-days)
log10 (trap-days)

Supplementary Files

This is a list of supplementary files associated with this preprint. Click to download.

- SupplementaryInformation.docx